OKU Fen Bilimleri Enstitüsü Dergisi
5(3): 1480-1493, 2022

OKU Journal of The Institute of Science and Technology, 5(3): 1480-1493, 2022

Osmaniye Korkut Ata Üniversitesi Fen Bilimleri Enstitüsü Dergisi

Osmaniye Korkut Ata University Journal of The Institute of Science and Technology

Determination of Tire Contact Stress and Deflection Distributions in a Layered Half-Space Using 3-D Boundary Element Method

İbrahim Özgür DENEME[1], Metin Hakan SEVERCAN[2*]

[1]Department of Civil Engineering, Aksaray University, 68100, Aksaray, Turkey
[2]Department of Civil Engineering, Niğde Ömer Halisdemir University, 51100, Niğde, Turkey

[1]https://orcid.org/0000-0001-5826-7187
[2]https://orcid.org/0000-0001-7320-8409
*Corresponding author: msever@ohu.edu.tr

Research Article

Article History:
Received: 13.12.2021
Accepted: 01.06.2022
Published online: 12.12.2022

Keywords:
Boundary element method
Elasto-statics
Fourier transform space
Pavement response
Layered half-space

ABSTRACT

In this study, the Boundary Element Method (BEM) was employed for the numerical determination of the response of a layered half-space. The material behaviour of the soil was assumed to be isotropic and linear elastic. The BEM was used in the Fourier transform space (FTS). The focus of this paper is to determine the stress and deflection distributions of interior points of a layered half-space. To achieve this aim, in this study, a computer program is developed for three-dimensional elastic or visco-elastic problems. The results of stress and deflection distributions in a layered half-space determined using boundary element formulation are presented in figures.

Tabakalı Zeminlerde Tekerlek Temas Gerilmesi ve Deplasman Dağılımlarının Üç Boyutlu Sınır Eleman Yöntemi ile Belirlenmesi

Araştırma Makalesi

Makale Tarihçesi:
Geliş tarihi: 13.12.2021
Kabul tarihi: 01.06.2022
Online Yayınlanma: 12.12.2022

Anahtar Kelimeler:
Sınır eleman yöntemi
Elasto-statik
Fourier dönüşüm uzayı
Üstyapı tepkisi
Tabakalı yarım uzay

ÖZ

Bu çalışmada, tabakalı bir yarım uzayın tepkisinin sayısal olarak belirlenmesi için sınır eleman yöntemi kullanılmıştır. Zeminin malzeme davranışının izotrop ve lineer elastik olduğu varsayılmıştır. Sınır eleman yöntemi, Fourier dönüşüm uzayında kullanıldı. Bu makalenin odak noktası, tabakalı bir yarım uzayın iç noktalarında oluşan gerilme ve deplasman dağılımlarının belirlenmesidir. Bu amaca ulaşmak için bu çalışmada, üç boyutlu elastik veya visko-elastik problemler için bir bilgisayar programı geliştirilmiştir. Sınır eleman formülasyonu kullanılarak belirlenen tabakalı bir yarım uzaydaki gerilme ve deplasman dağılımları şekillerde sunulmuştur.

To Cite: Deneme İÖ., Severcan MH. Determination of Tire Contact Stress and Deflection Distributions in a Layered Half-Space Using 3-D Boundary Element Method. Osmaniye Korkut Ata Üniversitesi Fen Bilimleri Enstitüsü Dergisi 2022; 5(3): 1480-1493.

1. Introduction

It is known that there are two different approaches for pavement design. One of them is rigid pavement design approach. Rigid pavement mainly consists of a concrete slab (with or without reinforcement) on the subgrade soil. Rigid concrete pavement distributes the vehicle axle loads by bending action on subgrade soil. Stress occurred in subgrade is generally lower than the strength of subgrade materials. However, vehicle loads produce much larger stress in concrete pavement material

than that of occurred on subgrade. Thus, stresses are carried by rigid pavement, and utilizing a concrete grade with sufficient tensile strength is generally adequate for design of rigid pavement (Yoder and Witczak, 1975). On the other hand, another approach is flexible pavement design. Flexible pavement distributes vehicle loads through its body and its total structure deflects under vehicle loads. A typical flexible pavement structure consists of mainly several layers of materials. Maximum stress is occurred on the surface of top layers, and stress is reduced on the lower part of materials. Determination of stress distribution in subgrade soil is important in design of flexible pavement. According to stress distribution within the flexible pavement, thickness of flexible pavement layers can be designed or for a certain thickness, selection of the materials with sufficient strength to be used in that layer can be specified.

Static or dynamic approaches can be used in the calculation of pavement response. Unlike dynamic analysis, inertial effects such as structural mass and damping ratios are ignored in static analysis. Subgrades of pavement can be modelled as an elastic or a viscoelastic homogeneous half-space with considering the influence of the load type, the velocity and frequency of the moving load (Kim and Roesset, 2003; Sun, 2006). In both analysis approaches, the pavement under vehicle loads can be considered as a homogeneous/layered elastic half-space. Vehicle load is applied on pavement through tires. Therefore, an acceptable description should be done for the contact stress between tires and pavement to obtain the true responses of pavement (Huang, 2004). Experimental measurements and numerical analysis such as finite element analyses have demonstrated that pressure distribution of the tyre-pavement contact is very complex (Hu and Sun, 2005; Hernandez and Al-Qadi, 2017). Some of the studies in the literature (Weissman, 1999; Hu and Sun, 2005) modelled contact area between tyre and pavement surface as a rectangle.

The numerical methods, such as Finite Element Method (FEM), BEM and coupling of FEM/BEM were used in solving pavement problems. With recent advancement of high-speed computers, the FEM become the most used numerical tool for the determination of stresses and strains. The first application of the FEM for the analysis of pavements may be found in reference (Duncan et al., 1968). Since then, several computer programs based on FEM have been developed for pavement analysis. Flexible pavements were modelled as elastic or viscoelastic layered half-spaces under static or dynamic stationary or moving loads (Mamlouk and Davies, 1984; Sousa et al., 1988; Siddharthan et al., 1998; Yoo and Al-Qadi, 2007; Al-Qadi et al., 2008; Vale, 2008; Khavassefat et al., 2012; Zheng et al., 2012; Lee et al., 2013; Beskou et al., 2016; Djellali et al., 2017; Castillo et al., 2019; Jiang et al., 2019). FEM/BEM combination is also used for determination of stresses and strains in flexible pavements (Pan and Atluri, 1995; François et al., 2007).

In FEM, a semi-infinite soil region should be modelled discretizing the whole volume presenting by brick elements having large number of degrees of freedom. In contrast the solution of a boundary value problem can be reduced by one dimension with the help of some integral equations in BEM (Brebbia and Dominguez, 1989; Banerjee, 1994; Yerli and Deneme, 2008; Deneme et al., 2009).

Hence, the BEM formulation requires smaller amount of data. The volume integrals can be carried to the boundary by using Dual Reciprocity Method (Partridge et al., 1992). The analytical expressions of the fundamental solutions can be determined for infinite medium (Mengi et al., 1994). Then the unknown boundary quantities (boundary tractions or displacements) can be calculated by using BEM. Besides, the response quantities at interior points can be computed numerically. The BEM studies applied in the literature can be found as calculation of the response of elastic/layered half-space under free field or on its surface moving loads (Payton, 1964; Grundmann et al., 1999; Lombaert et al., 2000; Rasmussen et al., 2001; Andersen and Nielsen, 2003; Beskou and Theodorakopoulos, 2011; Lu et al., 2018). According to authors' knowledge there is no BEM numerical work on the topic that calculates stress and deflection distributions in pavements.

In this study, the BEM was employed for the numerical determination of the response of pavements. The material behaviour of the soil was assumed to be linear elastic. The BEM was used in the FTS. The focus of this paper is to determine the stress and deflection distributions in interior points of a layered half-space. Therefore, in the static analysis, formulation was considered for stress and deflection distributions in a layered half-space, since the purpose of the study is to analyse the influence of the load model on the pavement response, with the BEM formulation adopted for pavement design.

2. Boundary Element Equation

In FTS, the governing equation (Brebbia and Dominguez, 1989; Banerjee, 1994; Mengi et al., 1994) is as follows for a body presented in Fig. 1.

$$\partial_j \tau_{ij} + f_i + \rho\omega^2 u_i = 0 \tag{1}$$

Boundary integral equation (BIE) in FTS is well established in literature (Brebbia and Dominguez, 1989; Banerjee, 1994; Mengi et al., 1994).

$$c_{lk} u_k(P) = \int_S G_{lk}(P,Q) t_k(Q) dS - \int_S H_{lk}(P,Q) u_k(Q) dS + \int_V G_{lk}(P,Q) f_k(Q) dV \tag{2}$$

where, G_{lk} and H_{lk} are first and second fundamental solutions; u_k, t_k and f_k are displacement, traction and body force components, respectively. c_{lk} is a constant depending on the location of source point P. Eqs. (1) and (2) were written in indicial notation form. The indices in these equations take the values from 1 to 3, for 3-D analysis.

The matrix form of BIE in Eq. (2) is presented in the following form:

$$\underline{c}\,\underline{u}(P) = \int_S \underline{G}(P,Q)\underline{t}(Q) dS - \int_S \underline{H}(P,Q)\underline{u}(Q) dS + \int_V \underline{G}(P,Q)\underline{f}(Q) dV \tag{3}$$

where the matrix values of $\underline{c}$ in Eq. (3) is given in Eq. (4).

$$\underline{c} = \begin{cases} \underline{I} & \text{If P is an interior point} \\ \underline{0} & \text{If P is on outside V} \\ \frac{1}{2}\underline{I} & \text{If P is on the boundary S} \end{cases} \tag{4}$$

The fundamental solution matrices ($\underline{G}$ and $\underline{H}$) have been established and found in the literature (Mengi et al., 1994).

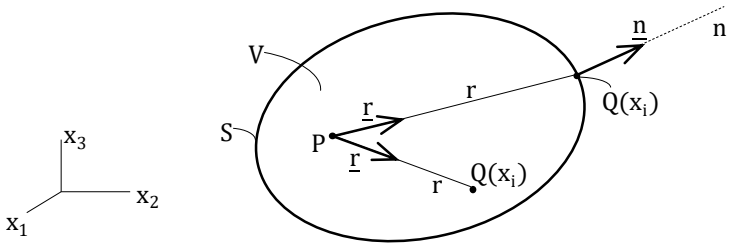

Fig. 1. Three dimensional body

3. Solution of Boundary Element Equation

For the determination of unknown boundary quantities, boundary element equation is solved numerically by discretizing the boundary into N boundary elements (Fig. 2). In the study, constant boundary elements are used for 3-D case.

After discretization, the boundary S is divided into small boundary elements, BIE, Eq. (3), can be obtained as follow for the node P_m of the m th boundary element,

$$\frac{1}{2}\underline{u}^m = \sum_{n=1}^{N} \underline{G}^{mn}\underline{t}^n - \sum_{n=1}^{N} \underline{H}^{mn}\underline{u}^n \quad (m = 1, \dots, N) \tag{5}$$

$$\underline{G}^{mn} = \int_{S_n} \underline{G}(P_m, Q)\,dS \tag{6}$$

$$\underline{H}^{mn} = \int_{S_n} \underline{H}(P_m, Q)\,dS \tag{7}$$

where S_n is the boundary of the n th element (Fig. 2). In Eq. (5), $\underline{u}^n$ and $\underline{t}^n$ are associated with the n th boundary element. Because the P_m node is not a corner point, $\underline{c}$ is taken as $\frac{1}{2}\,\underline{I}$ in analysis.

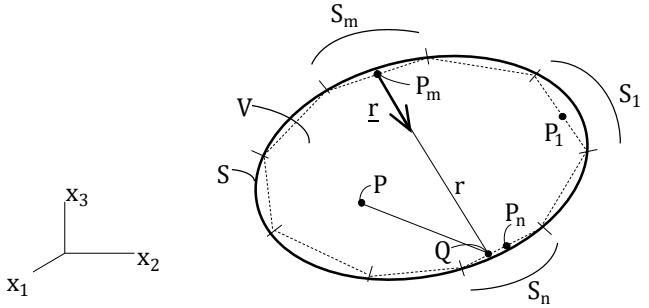

Fig. 2. Boundary element discretization of the body

Nodal displacements and traction components of a point can be defined as follows;

$$\underline{u}^n = \underline{u}(P_n) \tag{8}$$

$$\underline{t}^n = \underline{t}(P_n) \tag{9}$$

Using these formulations, the system equations of BEM can be obtained in matrix form as,

$$\underline{\tilde{H}}\,\underline{\tilde{u}} = \underline{\tilde{G}}\,\underline{\tilde{t}} \tag{10}$$

where;

$$\underline{\tilde{G}} = (\underline{G}^{mn}) \quad ; \quad \underline{\tilde{H}} = (\underline{H}^{mn} + \frac{1}{2}\underline{I}\delta_{mn}) \quad ; \quad \underline{\tilde{u}} = (\underline{u}^n) \quad ; \quad \underline{\tilde{t}} = (\underline{t}^n) \quad ; \quad (m=1,\ldots,N) \tag{11}$$

In these equations δ_{mn} is Kronecker's delta. The elements $\underline{G}^{mn}$ and $\underline{H}^{mn}$ may be computed numerically by using Gaussian quadrature integration formula. The unknown boundary quantities are obtained from the solution of Eq. (10) with the help of prescribed boundary conditions. Thus, the interior displacements and stresses can be computed numerically by using the boundary quantities.

3.1. Determination of Displacements at Interior Points

Having determined the boundary quantities, the displacements and stresses at an interior point P (Fig. 1) can be obtained using Eq. (2). It should be noted that the node P is an interior point. Hence, $\underline{c} = \underline{I}$ is used. When BIE, Eq. (2), in the absence of body force is written, then, the following equation can be obtained.

$$u_l(P) = \int_S G_{lk}(P,Q)t_k(Q)dS - \int_S H_{lk}(P,Q)u_k(Q)dS \tag{12}$$

There the fixed point P is an interior point. For the numerical solution of Eq. (12), when the boundary S is discretized into N boundary elements, and constant element formulation is used, then, Eq. (12) takes the form,

$$u_l(P) = \sum_{n=1}^{N} G_{lk}^n\, t_k^n - \sum_{n=1}^{N} H_{lk}^n u_k^n \tag{13}$$

where, G_{lk}^n and H_{lk}^n are expressed as in Eq. (14).

$$G_{lk}^n = \int_{S_n} G_{lk}(P,Q)dS \quad ; \quad H_{lk}^n = \int_{S_n} H_{lk}(P,Q)dS \tag{14}$$

Further, u_k^n and t_k^n denotes displacement and stress vector components of n^{th} element. Thus, Eq. (13) establishes the displacements at the interior point P in terms of boundary quantities. The integrals in Eq. (14) can be computed by using Gaussian quadrature numerical integration formula. Eqs. (12) and (14) were written in indicial notation form. The indices in these equations take the values from 1 to 3, for 3-D analysis.

3.2. Stresses Determination at Interior Points

In order to compute the stresses occurring at the interior point P, it is necessary to establish the constitutive equation together with the Eq. (2). The constitutive equation is given by Eq. (15).

$$\tau_{ij}(P) = c_{ijsl}\frac{\partial u_l}{\partial p_s}(P) \tag{15}$$

where, p_s's are the coordinates of point P, τ_{ij} (i, j = 1, 2, 3) are stress components, and c_{ijsl} is material constant. For isotropic materials, material constant value of c_{ijsl} is given in Eq. (16).

$$c_{ijsl} = \mu\left(\delta_{is}\delta_{jl} + \delta_{il}\delta_{js}\right) + \lambda\delta_{ij}\delta_{sl} \tag{16}$$

where λ is called as Lame constant.

To establish τ_{ij}'s, $\frac{\partial u_1}{\partial p_s}$ is to be computed. When the partial derivative of both sides of Eq. (12) with respect to the coordinates of the point P is obtained, and substituted in Eq. (15), the stress components at the point P can be obtained as given in Eq. (17).

$$\tau_{ij}(P) = \int_S D_{kij}(P,Q)t_k(Q)dS - \int_S S_{kij}(P,Q)u_k(Q)dS \tag{17}$$

where, $D_{kij}(P,Q)$ and $S_{kij}(P,Q)$ are described by Eq. (18).

$$D_{kij}(P,Q) = c_{ijsl}\frac{\partial G_{lk}(P,Q)}{\partial p_s}\ ;\ S_{kij}(P,Q) = c_{ijsl}\frac{\partial H_{lk}(P,Q)}{\partial p_s} \tag{18}$$

where, G_{lk} and H_{lk} denote the fundamental solutions. The indices in these equations take the values from 1 to 3, for 3-D analysis. G_{lk} and H_{lk} are, the first and the second fundamental solution for 3-D elasto-static case, given in Eq. (19).

$$G_{lk} = \frac{1}{16\pi\mu(1-\nu)r}\left[(3-4\nu)\delta_{lk} + r_l r_k\right]$$
$$H_{lk} = -\frac{1}{8\pi(1-\nu)r^2}\left[\frac{\partial r}{\partial_n}\{(1-2\nu)\delta_{lk} + 3r_l r_k\} + (1-2\nu)(n_l r_k - n_k r_l)\right] \tag{19}$$

where $\delta_{lk}, \nu, \mu\, n_k$ and n_l denote Kronecker delta, Poisson's ratio, shear modulus, outer unit normal vector components and unit vector components in $\overrightarrow{P_m Q}$ direction, respectively.

If the boundary element discretization of the body (Fig. 2) is taken into account, and the constant element formulation is used; the Eq. (17) takes the form as in the Eq. (20).

$$\tau_{ij}(P) = \sum_{n=1}^{N} D_{kij}^{n}\, t_k^n - \sum_{n=1}^{N} S_{kij}^{n} u_k^n \tag{20}$$

where,

$$D_{kij}^{n} = \int_{S_n} D_{kij}(P,Q)\,dS \quad ; \quad S_{kij}^{n} = \int_{S_n} S_{kij}(P,Q)\,dS \tag{21}$$

$\underline{D}^n$ and $\underline{S}^n$ coefficients in Eq. (21) can be computed by Gaussian quadrature numerical integration formula. Having known these coefficients and the boundary quantities $\underline{t}^n$ and $\underline{u}^n$, the stress values at the interior point P can be computed, using Eq. (20). The indices in these equations take the values from 1 to 3, for 3-D analysis. $\underline{D}^n$ and $\underline{S}^n$ coefficients involve $\underline{D}$ and $\underline{S}$ functions, defined in Eq. (18). These functions depend on elastic coefficients and fundamental solutions, and they can be defined by performing the operations indicated in Eq. (18). The $\underline{D}$ and $\underline{S}$ functions take forms for static analysis of isotropic elastic body are given in Eq. (22).

$$D_{kij} = \frac{1}{r^{\alpha}}\left\{(1-2\nu)\left[\delta_{ki}r_j + \delta_{kj}r_i - \delta_{ij}r_k\right] + \beta r_i r_j r_k\right\} \frac{1}{4\alpha\pi(1-\nu)}$$

$$S_{kij} = \frac{2\mu}{r^{\beta}}\left\{\beta\frac{\partial r}{\partial n}\left[(1-2\nu)\delta_{ij}r_k + \nu(\delta_{ik}r_j + \delta_{jk}r_i) - \gamma r_i r_j r_k\right] + \beta\nu\left(n_i r_j r_k\right) + (1-2\nu)\left(\beta n_k r_i r_j + n_j\delta_{ik} + n_i\delta_{jk}\right) - (1-4\nu)n_k\delta_{ij}\right\} \frac{1}{4\alpha\pi(1-\nu)} \tag{22}$$

where, values of α, β, γ are 2, 3 and 5, respectively.

3.3. BEM for a Composite Body

In this study, the boundary element formulation for an elastic body is presented. The composite body is consisting of two different regions, 1st region and 2nd region, with properties $(\mu_1, \rho_1, \nu_1, \text{etc})$ and $(\mu_2, \rho_2, \nu_2, \text{ etc.})$, respectively (see Fig. 3). The composite body has the boundaries S_1' and S_2' belonging to 1st region and 2nd region, respectively; and the interface S_c is common to both.

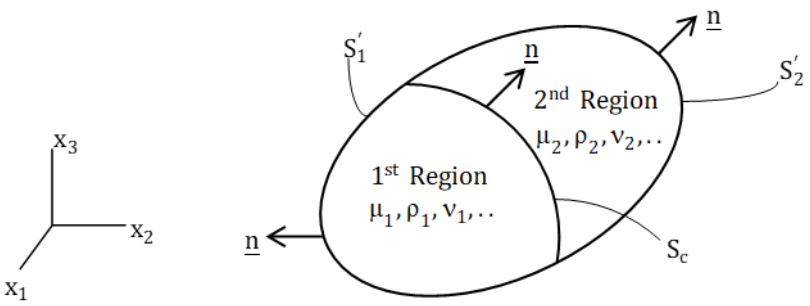

Fig. 3. A typical two-material composite body

The boundary element formulation of the composite body involves two-step, one is writing the system equation, Eq. (10), for 1st region and 2nd region; and the second one is, combining them so that the continuity conditions on the interface S_c is satisfied. In order to obtain the system equation for the two regions separately, the composite body is divided into two parts along the interface S_c boundary, as seen in Fig. 4. Accordingly, if the total boundaries of the first and second regions are denoted by S_1 and S_2, respectively, for these boundaries, the following equations can be obtained.

$$S_1 = S_1' \oplus S_c \quad ; \quad S_2 = S_2' \oplus S_c \tag{23}$$

The system equation, Eq. (10), for 1st region can be written as,

$$\left[\, \underline{\tilde{H}}_1 \quad \underline{\tilde{H}}_{1c} \,\right] \begin{bmatrix} \underline{\tilde{u}}_1 \\ \underline{\tilde{u}}_{c1} \end{bmatrix} = \left[\, \underline{\tilde{G}}_1 \quad \underline{\tilde{G}}_{1c} \,\right] \begin{bmatrix} \underline{\tilde{t}}_1 \\ \underline{\tilde{t}}_{c1} \end{bmatrix} \tag{24}$$

Similarly, the system equation, Eq. (10), for 2nd region can be written as,

$$\left[\, \underline{\tilde{H}}_2 \quad \underline{\tilde{H}}_{2c} \,\right] \begin{bmatrix} \underline{\tilde{u}}_2 \\ \underline{\tilde{u}}_{c2} \end{bmatrix} = \left[\, \underline{\tilde{G}}_2 \quad \underline{\tilde{G}}_{2c} \,\right] \begin{bmatrix} \underline{\tilde{t}}_2 \\ \underline{\tilde{t}}_{c2} \end{bmatrix} \tag{25}$$

Boundary conditions on S_1' and S_2' are already given in Eqs. (8) and (9). On the other hand, boundary conditions for continuity conditions on the interface S_c can be defined as follows;

$$\underline{u}_{c1} = \underline{u}_{c2} \quad ; \quad \underline{t}_{c1} = -\underline{t}_{c2} \tag{26}$$

When Eqs. (24) and (25) are combined, in the view of Eqs. (26), the system equations for the two-material composite body can be obtained as,

$$\begin{bmatrix} \tilde{\underline{H}}_1 & 0 & \tilde{\underline{H}}_{1c} \\ 0 & \tilde{\underline{H}}_2 & \tilde{\underline{H}}_{2c} \end{bmatrix} \begin{bmatrix} \tilde{\underline{u}}_1 \\ \tilde{\underline{u}}_2 \\ \tilde{\underline{u}}_c \end{bmatrix} = \begin{bmatrix} \tilde{\underline{G}}_1 & 0 & \tilde{\underline{G}}_{1c} \\ 0 & \tilde{\underline{G}}_2 & \tilde{\underline{G}}_{2c} \end{bmatrix} \begin{bmatrix} \tilde{\underline{t}}_1 \\ \tilde{\underline{t}}_2 \\ \tilde{\underline{t}}_c \end{bmatrix} \tag{27}$$

where,

$$\underline{u}_{c1} = \underline{u}_c \quad ; \quad \underline{t}_{c1} = \underline{t}_c \tag{28}$$

The solution of the system equation in Eq. (27) determines the unknown boundary quantities on S_1 and S_2 as well as unknown interface displacements and tractions. Having known them, the interior displacements and stresses can be computed numerically by using the boundary quantities.

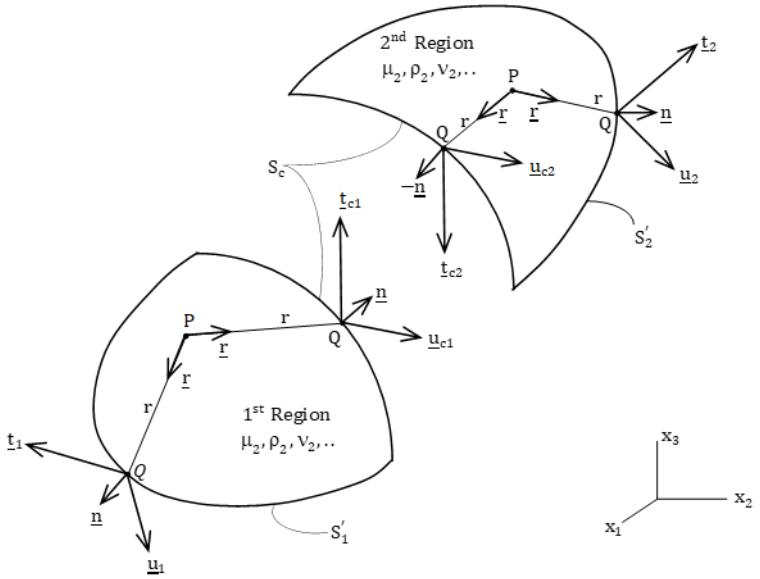

Fig. 4. Free body diagrams of 1st region and 2nd region of composite body

4. Numerical Examples

In this study, a computer program has been prepared for the mentioned BEM formulation. In this program, all calculations are performed in FTS. By using this computer program, a circular rigid foundation subjected to uniformly distributed unit load on the ground, given in Fig. 5, consisting of a half-space with an elastic layer on it, is considered and solved as a problem. In the analysis Poisson's ratio was taken as 0.5 in both regions. The elasticity modulus ratio (E_1/E_2) of both regions is 1, 2, 5, 10, 20, 50 and 100 are used as the modulus of elasticity values. The static analysis is used with the help of the prepared program. The nondimensional stress distributions in the layers were obtained at the points A(0,5a, 0, 3a), B (a, 0, 3a), C(1,1a, 0, 3a) and D(2a, 0, 3a) along the x_3 axis. The analysis is carried out in nondimensional space. The results, which were obtained using boundary element formulation are presented in Figs. 6-9. In the analysis of these problems, mesh truncation is used and the fundamental solutions are integrated with Gaussian quadrature formulas.

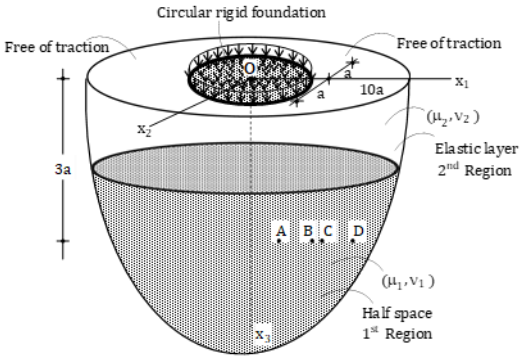

Fig. 5. Composite body under uniformly distributed circular load

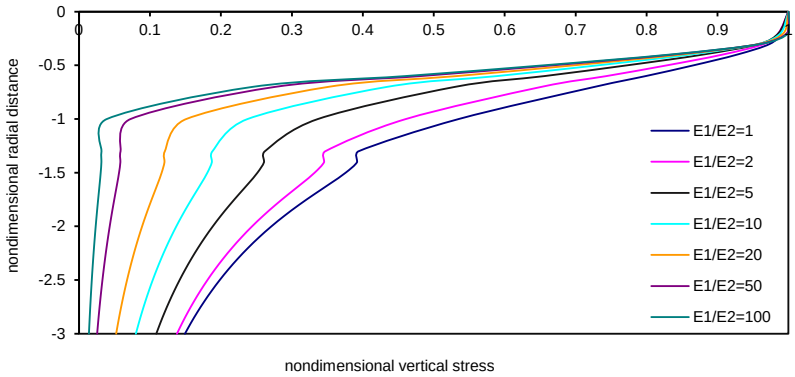

Fig. 6. Variation of vertical stress with radial distance at point A

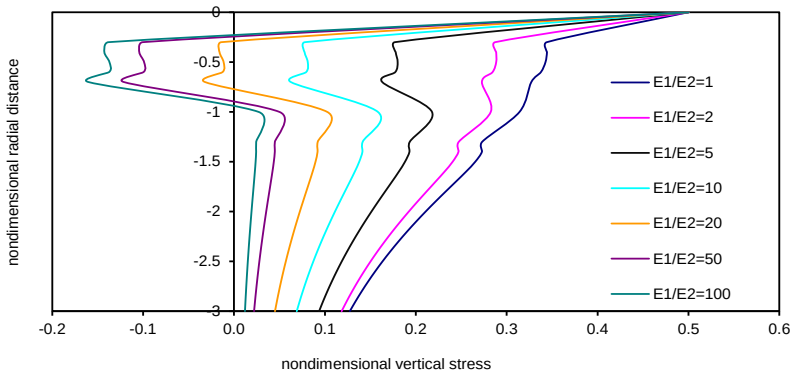

Fig. 7. Variation of vertical stress with radial distance at point B

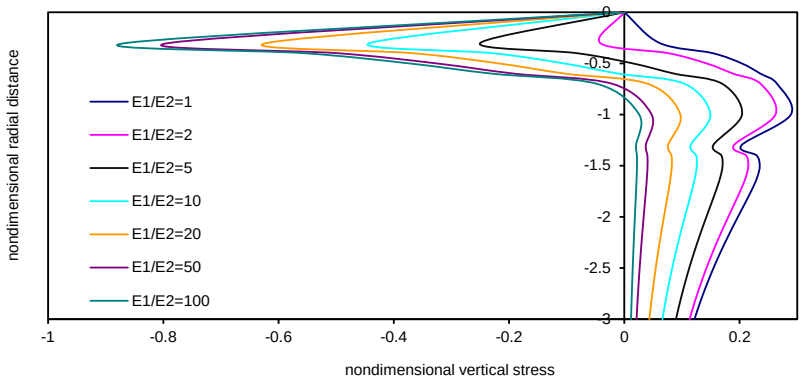

Fig. 8. Variation of vertical stress with radial distance at point C

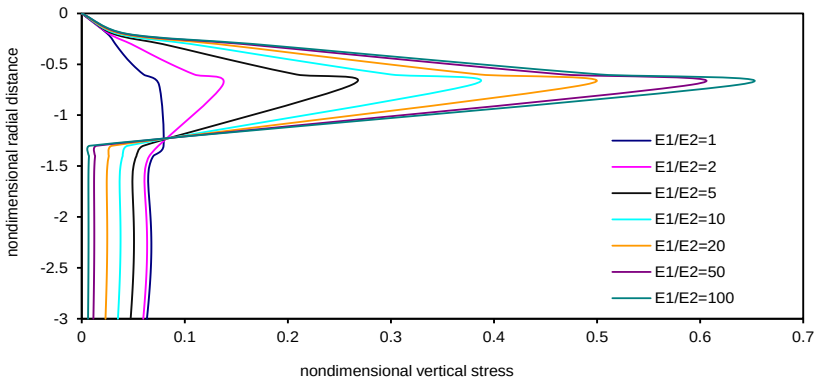

Fig. 9. Variation of vertical stress with radial distance at point D

5. Conclusions

In the study, 3-D boundary element formulation is presented. Based on the formulation, a general-purpose computer program is developed, and it is applied to pavement design problems. By using this computer program, a circular rigid foundation subjected to uniformly distributed unit load on the ground, consisting of a half-space with an elastic layer on it, is considered and solved as a problem. In this program, all calculations are performed in FTS. In the analysis of this problem, mesh truncation is used and the fundamental solutions are integrated with Gaussian quadrature formulas. The static analysis was considered for stress and deflection distributions in a layered half-space, since the purpose of the study is to analyse the influence of the load model on the pavement response, with the BEM formulation adopted for pavement design. The obtained results from the BEM formulation are presented in the figures. The results presented at Figures indicate that the formulation presented in this study can be used with good confidence in the analysis of pavement design problems consisting of a half-space with/without an elastic layer on it.

Conflict of Interest Statement

The authors of the article declare that there is no conflict of interest.

Contribution Rate Statement Summary of Researchers

The authors declare that they have contributed equally to the article.

References

Al-Qadi IL., Wang H., Yoo PJ., Dessouky SH. Dynamic analysis and in situ validation of perpetual pavement response to vehicular loading. Transportation Research Record 2008; 2087: 29–39.

Andersen L., Nielsen SRK. Boundary element analysis of the steady-state response of an elastic half-space to a moving force on its surface. Engineering Analysis with Boundary Elements 2003; 27: 23–38.

Banerjee PK. The boundary element methods in engineering. London: McGraw-Hill Book Company; 1994.

Beskou ND., Hatzigeorgiou GD., Theodorakopoulos DD. Dynamic inelastic analysis of 3-D flexible pavements under moving vehicles: A unified FEM treatment. Soil Dynamics and Earthquake Engineering 2016; 90: 420–431.

Beskou ND., Theodorakopoulos DD. Dynamic effects of moving loads on road pavements: A review. Soil Dynamics and Earthquake Engineering 2011; 31: 547–567.

Brebbia CA., Dominguez J. Boundary elements an introductory course. Southampton: Computational Mechanics Publications; 1989.

Castillo D., Gamez A., Al-Qadi I. Homogeneous versus heterogeneous response of a flexible pavement structure: strain and domain analyses. Journal of Engineering Mechanics 2019; 145: 04019068.

Deneme IO., Yerli HR., Severcan MH., Tanrikulu AH., Tanrikulu AK. Use and comparison of different types of boundary elements for 2D soil-structure interaction problems. Advances in Engineering Software 2009; 40: 847–855.

Djellali A., Houam A., Saghafi B., Hamdane A, Benghazi Z. Static analysis of flexible pavements over expansive soils. International Journal of Civil Engineering 2017; 15: 391–400.

Duncan JM., Monismith CL., Wilson EL. Finite element analyses of pavements. Highway Research Board 1968; 38: 18–33.

François S., Pyl L., Masoumi HR., Degrande G. The influence of dynamic soil-structure interaction on traffic induced vibrations in buildings. Soil Dynamics and Earthquake Engineering 2007; 27: 655–674.

Grundmann H., Lieb M., Trommer E. The response of a layered half-space to traffic loads moving along its surface. Archive of Applied Mechanics 1999; 69: 55–67.

Hernandez JA., Al-Qadi IL. Tire–pavement interaction modelling: hyperelastic tire and elastic pavement. Road Materials and Pavement Design 2017; 18: 1067–1083.

Hu XD., Sun LJ. Measuring tire ground pressure distribution of heavy vehicle. Journal of Tongji

University 2005; 33: 1443–1448.

Huang YH. Pavement design and analysis. New Jersey: Pearson Prentice Hall; 2004.

Jiang X., Zeng C., Gao X., Liu Z., Qiu Y. 3D FEM analysis of flexible base asphalt pavement structure under non-uniform tyre contact pressure. International Journal of Pavement Engineering 2019; 20: 999–1011.

Khavassefat P., Jelagin D., Birgisson B. A computational framework for viscoelastic analysis of flexible pavements under moving loads. Materials and Structures 2012; 45: 1655–1671.

Kim SM., Roesset JM. Dynamic response of a beam on a frequency-independent damped elastic foundation to moving load. Canadian Journal of Civil Engineering 2003; 30: 460–467.

Lee JH., Kim JK., Tassoulas JL. Dynamic analysis of a layered half-space subjected to moving line loads. Soil Dynamics and Earthquake Engineering 2013; 47: 16–31.

Lombaert G., Degrande G., Clouteau D. Numerical modelling of free field traffic-induced vibrations. Soil Dynamics and Earthquake Engineering 2000; 19: 473–488.

Lu YJ., Wang LJ., Yang Q., Ren JY. Analysis of asphalt pavement mechanical behaviour by using a tire-pavement coupling model. International Journal of Simulation Modelling 2018; 17: 245–256.

Mamlouk MS., Davies TG. Elasto-dynamic analysis of pavement deflections. Journal of Transportation Engineering 1984; 110: 536–550.

Mengi Y., Tanrikulu AH., Tanrikulu AK. Boundary element method for elastic media: an introduction. Ankara: METU Press; 1994.

Pan G., Atluri SN. Dynamic response of finite sized elastic runways subjected to moving loads: A coupled BEM/FEM approach. International Journal for Numerical Methods in Engineering 1995; 38: 3143–3166.

Partridge PW., Brebbia CA., Wrobel LC. The dual reciprocity boundary element method. Southampton: Computational Mechanics Publications; 1992.

Payton RG. An application of the dynamic Betti-Rayleigh reciprocal theorem to moving-point loads in elastic media. Quarterly of Applied Mathematics 1964; 21: 299–313.

Rasmussen KM., Nielsen SRK, Kirkegaard PH. Boundary element method solution in the time domain for a moving time-dependent force. Computers and Structures 2001; 79: 691–701.

Siddharthan RV., Yao J., Sebaaly PE. Pavement strain from moving dynamic 3D load distribution. Journal of Transportation Engineering 1998; 124: 557–566.

Sousa BJ., Lysmer J., Chen SS., Monismith CL. Effects of dynamic loads on performance of asphalt concrete pavements. Transportation Research Record 1988; 1207: 145–168.

Sun L. Analytical dynamic displacement response of rigid pavements to moving concentrated and line loads. International Journal of Solids and Structures 2006; 43: 4370–4383.

Vale C. Influence of vertical load models on flexible pavement response - An investigation. International Journal of Pavement Engineering 2008; 9: 247–255.

Weissman SL. Influence of tire-pavement contact stress distribution on development of distress mechanisms in pavements. Transportation Research Record 1999; 1655: 161–167.

Yerli HR., Deneme IO. Elastodynamic boundary element formulation employing discontinuous curved elements. Soil Dynamics and Earthquake Engineering 2008; 28: 480–491.

Yoder EJ., Witczak MW. Principles of pavement design, Second Edition. 1975.

Yoo PJ., Al-Qadi IL. Effect of transient dynamic loading on flexible pavements. Transportation Research Record 2007; 1990: 129–140.

Zheng L., Hai-lin Y., Wan-ping W., Ping C. Dynamic stress and deformation of a layered road structure under vehicle traffic loads: Experimental measurements and numerical calculations. Soil Dynamics and Earthquake Engineering 2012; 39: 100–112.